Tree Physiology 35, 1206–1222
doi:10.1093/treephys/tpv097

Research paper

Non-structural carbon dynamics and allocation relate to growth rate and leaf habit in California oaks

Susan Trumbore[1,2,3], Claudia I. Czimczik[1], Carlos A. Sierra[2], Jan Muhr[2] and Xiaomei Xu[1]

[1]Department of Earth System Science, University of California, Irvine, Irvine, CA 92697-3100, USA; [2]Department of Biogeochemical Processes, Max-Planck-Institute for Biogeochemistry, 07701 Jena, Germany; [3]Corresponding author (trumbore@bgc-jena.mpg.de)

Received May 3, 2015; accepted August 17, 2015; published online October 8, 2015; handling Editor Lucas Cernusak

Trees contain non-structural carbon (NSC), but it is unclear for how long these reserves are stored and to what degree they are used to support plant activity. We used radiocarbon (^{14}C) to show that the carbon (C) in stemwood NSC can achieve ages of several decades in California oaks. We separated NSC into two fractions: soluble (~50% sugars) and insoluble (mostly starch) NSC. Soluble NSC contained more C than insoluble NSC, but we found no consistent trend in the amount of either pool with depth in the stem. There was no systematic difference in C age between the two fractions, although ages increased with stem depth. The C in both NSC fractions was consistently younger than the structural C from which they were extracted. Together, these results indicate considerable inward mixing of NSC within the stem and rapid exchange between soluble and insoluble pools, compared with the timescale of inward mixing. We observed similar patterns in sympatric evergreen and deciduous oaks and the largest differences among tree stems with different growth rates. The ^{14}C signature of carbon dioxide (CO_2) emitted from tree stems was higher than expected from very recent photoassimilates, indicating that the mean age of C in respiration substrates included a contribution from C fixed years previously. A simple model that tracks NSC produced each year, followed by loss (through conversion to CO_2) in subsequent years, matches our observations of inward mixing of NSC in the stem and higher ^{14}C signature of stem CO_2 efflux. Together, these data support the idea of continuous accumulation of NSC in stemwood and that 'vigor' (growth rate) and leaf habit (deciduous vs evergreen) control NSC pool size and allocation.

Keywords: carbon isotope composition, stable carbon isotope, stem CO_2 efflux, sugar.

Introduction

Trees transport, accumulate and store photosynthetic assimilates as non-structural carbon (NSC) (Chapin et al. 1990, Kozlowski 1992, Dietze et al. 2014). This comprises a variety of compounds, including soluble (mainly sugars) and insoluble (starch and lipids) phases (Li et al. 2002, Hoch et al. 2003). Among other functions (Körner 2003), storing NSC is a mechanism for plants to survive and initiate growth at the end of dormant seasons and to re-grow tissues following herbivory or catastrophic damage, e.g., by fire (Mooney and Hays 1973, Langley et al. 2002, Wong et al. 2005). In trees, NSC dynamics are largely controlled by sink strength (Körner 2003) and accumulate when growth sinks are limited, e.g., during dormant seasons (Richardson et al. 2013), by cold (Hoch and Körner 2003) or drought (Tschaplinski and Hanson 2003, Hartmann et al. 2013*a*), as well as by pollution (Grulke et al. 2001) or nutrient stress (Ericsson et al. 1996). During drought, NSC accumulates in above-ground tissues when transport to sink tissues is limited (Hartmann et al. 2015). In addition to its role in the carbon (C) budget of trees, NSC also plays a role in supporting hydraulic function during drought or freezing conditions and as trees grow in height (Sala et al. 2012, Sevanto et al. 2014).

In forest ecosystems, NSC represents a significant C pool as NSC production, loss and storage are major terms in the annual C balance (Körner 2003). The annual demand for NSC, if expressed

on a whole-tree basis (or extrapolated to an areal average), represents a flux of C that is similar to (or greater than) annual leaf litterfall (Barbaroux and Breda 2002, Hoch et al. 2003, Würth et al. 2005).

In mature tree tissues, NSC concentrations range from ~2 to 20% on a dry weight basis (Barbaroux et al. 2003, Körner 2003). Non-structural carbon concentrations vary seasonally, among organs and between species (Gholz and Cropper 1991, Richardson et al. 2013, 2015), but are usually high in leaves, branches and roots and lower in stems. The greater overall mass contained in stems and coarse roots, however, means that most of NSC is in these organs (Barbaroux et al. 2003, Richardson et al. 2015). Year-to-year variations in NSC stocks, reflecting annual imbalances in C supply and demand, have been suggested to play a major role in interannual variations of stand-level C balance (Tschaplinski and Hanson 2003) and may be the cause of a lack of observed correlation between annual tree ring growth and stand-level gross primary productivity (Rocha et al. 2006, Richardson et al. 2013).

We know little about if and how NSC dynamics vary with tree life traits, such as evergreen vs deciduous or ring-porous vs diffuse-porous wood, and along climate gradients. A key measure of the dynamics of the NSC pool is the age of the C contained in NSC reserves and/or the age of the NSC used to fuel growth or respiration. Hoch et al. (2003) measured NSC in stemwood and found little seasonal variation with the variable timing of source and sink strengths, suggesting that in mature trees the turnover time of the NSC pool exceeds several seasons. Hoch et al. (2003) also showed that NSC in one oak (*Quercus petraea*) declined with sapwood depth in the stem, indicating that either inward mixing is rapid or NSC can be preserved over the period when wood tissues remain conductive. Keel et al. (2007) showed that even after 4 years of continuous isotope labeling of photoassimilates, storage reserves that pre-dated the label were still used to grow new structural tissues. Measurements of radiocarbon (^{14}C) in NSC extracted from the outermost stemwood from three temperate forest species (maple, oak and hemlock) showed that on average C in these pools was fixed several years up to a decade ago in mature temperate forest trees (Richardson et al. 2013, 2015, Carbone et al. 2013).

Evidence that several-years-old, stored reserves contribute to respiration comes from measurements of the mean age of C being respired from roots (Czimczik et al. 2006, Schuur and Trumbore 2006, Carbone and Trumbore 2007) and emitted from tree stems (Carbone et al. 2013, Muhr et al. 2013) and post-disturbance growth tissues (Vargas et al. 2009, Carbone et al. 2013). Pulse-chase labeling studies of whole trees (Carbone et al. 2007, Kuptz et al. 2011) and ^{14}C measurements (Muhr et al. 2013) also show the contributions of older C to respiration and to the growth of new tissues (Gaudinski et al. 2009, Vargas et al. 2009). These studies hint that there is a slower cycling pool of NSC that is used to support respiration and recovery from damage and emphasize the potential role of NSC in stand-level C balance. A major question remains as to the role of these several-years- to decades-old NSC reserves in supporting respiration overall, or if the contribution reflects predominantly periods when C demand exceeds supply (e.g., Sala et al. 2012).

Here, we report ^{14}C measurements of NSC as a function of depth into the tree stem for sympatric evergreen and deciduous Mediterranean oaks from five sites in California (CA), USA. We compare the mean 'age' of C in cellulose and soluble and insoluble NSC for sympatric oak trees with contrasting life strategies (deciduous vs evergreen) and receiving varying amounts of winter rain. We also report the ^{14}C signature of carbon dioxide (CO_2) emitted year-round from the same tree stems and use a model to quantify the relative roles of mixing and consumption as a function of radial distance within the stem that can explain both observations.

Materials and methods

Research sites

We studied mature individuals of five native tree species with two different life strategies along a north-to-south transect in CA, USA (Table 1): two evergreen (CA live oak (*Quercus agrifolia* Née) and interior live oak (*Quercus wislizeni* A. DC.)) and three winter-deciduous (valley oak (*Quercus lobata* Née), blue oak (*Quercus douglasii* Hook. & Arn.) and CA sycamore (*Platanus racemosa* Nutt.)). The sycamore stand is the same one investigated by McCarthy and Pataki (2010) in a comparison of water usage by native and urban trees in Southern CA.

Our research sites are nature reserves located along a precipitation gradient; mean annual precipitation (MAP) decreases from north to south by 50% (Table 1). The climate is Mediterranean with hot, dry summers and highly variable amounts of winter rain (November–April in Southern CA and October–May in central and northern CA) (Abatzoglou et al. 2009). The growing season is during the boreal summer (dry season). The mean annual temperature (MAT) is ~17 °C, but lower at Hastings, which receives coastal fog. Here, MAT and its seasonal amplitude as well as MAP are lower than expected from the transect position.

Stemwood sampling

At each site, we sampled stemwood at the end of winter (wet season) and summer (dry season) in 2008 (Table 1). We measured the diameter at breast height (1.3 m) of each tree using a diameter tape and estimated the height with a tangent height gage (Forestry Suppliers Inc., Jackson, MS, USA).

From most trees, we extracted stem cores of 7–20 cm length using 4.3 mm diameter, 36 cm length increment borers (Haglöf, Madison, MS, USA). The wood of some live and blue oaks was too dense to core, so instead, we cut out rectangular

Table 1. Overview of study sites and activities in CA, USA. Stemwood was sampled from three to six trees per species per site, and CO_2 was sampled from five trees per species per site. The Quail Ride, Sedgwick, Hastings and Emerson Reserves are part of the University of California's Natural Reserve System (http://nrs.ucop.edu/). Starr Ranch is a US National Audubon Society sanctuary (http://www.starrranch.org/). n.m., not measured; a.s.l., above sea level.

Research site (weather station)	Latitude/longitude (N/W)	Elevation[1] (m a.s.l.)	MAP[2] (dry/wet) (mm)	MAT[3] (dry/wet) (°C)	Species[4]	Height[5] (m)	dbh[6] (m)	Wood sampling (dd/mm/yy)	Chamber installed (dd/mm/yy)
Quail Ridge Reserve (Winters)	38°28′59.16″/122°8′57.84″	157 (22)	580 (12/568)	17 (25/13)	***Q. wislizeni***	17.5 (2.2)	0.3 (0.01)	26/02/08–27/02/08, 29/08/08	n.m.
					Q. douglasii	19.3 (2.3)	0.5 (0.03)		
					Q. lobata	23.3 (2.9)	0.8 (0.1)		
Sedgwick Reserve (Los Olivos)	34°40′31.62″/120°2′26.43″	367 (24)	555 (10/546)	17 (22/14)	***Q. agrifolia***	14.7 (1.4)	1.0 (0.1)	15/02/08–20/02/08, 24/08/08–25/08/08	18/08/10
					Q. douglasii	15.8 (1.3)	0.6 (0.1)		
					Q. douglasii × *lobata*	16.6 (0.3)	0.6 (0.04)		
					Q. lobata	14.2 (1.5)	0.7 (0.05)		
Hastings Natural History Reservation (Carmel Valley)	36°24′28.97″/121°35′34.51″	547 (17)	517 (17/500)	14 (16/13)	***Q. agrifolia***	15.9 (1.3)	0.6 (0.1)	23/02/08–25/02/08, 26/08/08–27/08/08	n.m.
					Q. wislizeni	11.7 (0.4)	0.3 (0.1)		
					Q. douglasii	15.0 (0.7)	0.5 (0.1)		
					Q. lobata	15.9 (1.7)	0.6 (0.1)		
Starr Ranch (Mission Viejo)	33°37′50.92″/117°33′45.26″	267 (0)	356 (31/326)	18 (21/15)	***Q. agrifolia***	19.4 (1.6)	0.4 (0.1)	22/01/08, 30/09/08	10/08/10
					P. racemosa	n.m.	n.m.	n.m.	
Emerson Oaks Reserve (Temecula)	33°28′0.00″/117°2′21.98″	473 (15)	290 (28/262)	18 (23/13)	***Q. agrifolia***	14.8 (2.5)	0.6 (0.04)	05/02/08, 10/10/08	n.m.

[1]Average (SD).
[2]Mean annual, dry and wet season precipitation.
[3]Mean annual, dry and wet season temperature at nearby weather stations (www.weather.com, 2010); dry season is defined as mean monthly precipitation <10 mm.
[4]Bold font indicates evergreen and normal font indicates winter deciduous.
[5]Average (SE).
[6]Diameter at 1.3 m height, average (SE).

(~5 × 3 cm^2 × 2 cm deep) chunks of sapwood using a hammer and chisel. All samples were taken on the northern side of the stem during the first and 10 cm further west during the second sampling. Fresh samples were stored in plastic straws (cores) or bags (chunks) on ice in a cooler, microwaved for 1 min within 4–6 h of sampling (Li et al. 2002) and frozen at −20 °C. Tools were cleaned with water and ethanol and dried after each sample and with dish liquid, water and then ethanol between sites. Tree wounds were dressed with commercially available pruning sealant.

Frozen samples were manually cut into 1–2 cm intervals (starting below the bark), dried in a speedvac drier (SC200 with RT400 cold trap, Savant, Thermo Fisher Scientific, Waltham, MA, USA) and manually chopped into flakes with a scalpel. For soluble NSC, wood grinding decreases the preparation time and may increase the extraction efficiency (Richardson et al. 2015). The extraction of insoluble NSC may fail, however, if ethanol used during the cleaning step (see Insoluble NSC) is not fully removed.

Stem-emitted CO_2 sampling

At two sites, we quantified and collected CO_2 emissions from tree stems from August 2010 to July 2011 (Table 1) using polypropylene chambers (2.93 l covering 256 cm^2 of the stem; for details see Muhr et al. (2013)). The chambers were attached to the tree with hot glue, which was sealed on the outside with single component, elastic marine adhesive- and sealing-compound based on silylmodified polymers (Nautiflex, OASE GmbH, Oerel-Barchel, Germany), and secured with nylon cinching straps. To ensure a leak-tight fit, chambers were fixed onto the cork cambium of the oaks (cork was removed in a rectangle roughly the size of the chamber frame), but directly onto the sycamore bark. To prevent overheating, chambers were covered with a reflective aluminum blanket. To exclude fauna, chamber openings were covered with a metal screen when not in use.

Prior to measuring fluxes, the chambers were vented for ≥1 h by removing the screens. Then, the rate of CO_2 emission was measured by circulating air in a closed loop between the chamber and an infrared CO_2 analyzer (Li-820, LI-COR Environmental, Lincoln, NE, USA). The temperature inside the chamber was monitored with a thermocouple. We measured the increase of CO_2 inside the chamber for a period of ~10 min and used linear regression of concentration vs time together with the volume and surface area enclosed by the chamber to estimate the rate of stem CO_2 efflux.

Subsequently, the chamber ports were closed, and the chamber was covered with a reflective aluminum shield. We allowed CO_2 inside the chamber to accumulate for 1–14 h to yield ≥0.5 mg C. To minimize pressure fluctuations during sampling, one port of the chamber was opened to the atmosphere via a soda lime-filled tube. The other chamber port was connected to a pre-evacuated stainless steel canister (0.5 or 2 l) via a series of stainless steel capillaries that restricted the flow rates to ~0.07 l min^{-1} (10 cm length × 0.01 ID, 150 cm × 0.03 ID, Thermo Fisher Scientific) and a magnesium perchlorate tube for drying.

Ambient CO_2 sampling

As a proxy for the ^{14}C signature of growing season, daytime atmospheric CO_2, we collected green leaves of two annual plants at each sampling. Leaf samples were oven-dried at 60 °C, homogenized and 2–4 mg was weighed into pre-baked (900 °C for 2 h) quartz tubes (6 mm OD, 13 cm length). We also collected ambient air during each stem CO_2 emission sampling event by slowly filling an evacuated 6 l stainless steel canister (SiloCan, Restek Corporation, Bellefonte, PA, USA) via the same capillaries and drying tube described for stem CO_2 sampling mentioned earlier.

Isolation of soluble and insoluble NSC and structural C pools

A major initial study goal was to develop methods to extract and analyze NSC pools and determine how accurately we can measure their ^{14}C signature. Improved methods based on these initial tests were reported in Carbone et al. (2013) and Richardson et al. (2013, 2015). Although a large number of methods for measuring NSC exist, methods and results differ widely among methods and laboratories (Richter et al. 2009). Additional difficulties are introduced when isolating NSC for the analysis of natural abundance levels of ^{14}C (1 ppt or smaller), which requires the physical isolation of pools, but inhibits the use of destructive methods such as compound-specific enzyme digestion (Li et al. 2002, Gomez et al. 2007) or chromatography (Raessler 2011). In addition, use of C-containing solvents can introduce extraneous C into the sample, and methods must be tested to evaluate the extent of such contamination.

We isolated three C fractions from each wood core increment subsequentially, which we refer to as 'soluble' ('sugars')—extracted with methanol : water (Gomez et al. 2007), 'insoluble' ('starch')—extracted with HCl (Richter et al. 2009) and 'structural' ('cellulose')—via the acid–base–acid (ABA) method (Santos and Ormsby 2013). Because we used operationally defined fractionation procedures, the extracts can contain a range of compounds. We did attempt to characterize the sugar content of the soluble fraction (discussed subsequently). The chemical composition of wood subjected to the ABA method is discussed in Gaudinski et al. (2005); ^{14}C in wood treated with this method is indistinguishable from α-cellulose and differences in ^{14}C between structural C and NSC solely reflect 'age'.

The extraction procedure was performed in sequence from the same sample in batches of nine samples and two standards (ANU sucrose (IAEA-C6) and in-house 'French fries' starch standard). Approximately 300 mg of sample was weighed into a 50 ml reusable glass centrifugation tube (Kimble, Thermo Fisher Scientific). All glassware was pre-baked at 550 °C for 4 h prior to use, all surfaces were covered with aluminum foil and all stainless steel tools were cleaned with ethanol and thoroughly dried.

Soluble NSC The soluble NSC pool was extracted from wood with 30 ml high-performance liquid chromatography (HPLC)-grade methanol : MilliQ (MQ) H_2O (1 : 1, v : v) using vortex shaking followed by horizontal shaking for 1 h at room temperature, modifying the procedure of Gomez et al. (2007). After centrifugation, the supernatant containing the soluble NSC was transferred into a new 50 ml tube and speedvac-dried. To remove all traces of methanol-derived C (determined using tests from dissolving and isolating ANU sucrose), soluble NSC was twice re-dissolved in 10 ml MQ H_2O and vacuum-dried. The purified extract was then re-dissolved in 10 ml MQ H_2O. In batches of 0.5–2 ml, a subsample (0.5–5 ml extract, yielding 0.3–1.2 mg C) was transferred to a quartz combustion tube (9 mm OD, 12 cm length) and speedvac-dried. The remaining extract was refrigerated.

The soluble NSC pool contained a number of compounds beyond the expected simple sugars. These included pigmented compounds, probably tannins. Attempts to measure the content of sucrose, glucose and fructose in the soluble fraction using enzymatic techniques based on colorimetry following Gomez et al. (2007) were unsuccessful, except for standards—likely as a consequence of the high tannin content of the samples. After many months of refrigerated storage, a subset of the stored samples was measured by HPLC (ICS 3000, Dionex, Thermo Fisher Scientific) (Raessler 2011), from which it was determined that ~50% of the measured C in our samples was in the form of glucose, sucrose and fructose (see Figure S1 available as Supplementary Data at *Tree Physiology* Online).

Insoluble NSC The wood was further extracted by boiling in 30 ml ultrapure ethanol for 30 min in a block heater (VWR, Radnor, PA, USA). The supernatant was removed with a disposable, plastic-extended fine tip transfer pipette (Samco Scientific, Thermo Fisher Scientific) and discarded. This cleaning step was repeated until the supernatant was clear and colorless.

Then, the insoluble NSC pool was extracted (Richter et al. 2009) in 10 ml of 20% HCl at 50 °C for 30 min and then at room temperature for 8–12 h (overnight). After centrifugation, the supernatant containing the insoluble NSC was transferred to a new 50 ml tube and refrigerated. This extraction was repeated, and the supernatant combined with the first acid extract (yielding ≤20 ml of the liquid). Insoluble NSC was precipitated from the acid extracts by adding 30 ml HPLC-grade ethanol (yielding ≤50 ml) and letting the mixture stand overnight. Following centrifugation, the supernatant was discarded. To remove traces of extraneous C from the ethanol, the 'entire' insoluble NSC fraction (precipitate) was twice re-dissolved in 10 ml MQ water and reduced to ~0.5–1 ml using the speedvac drier and finally re-dissolved and transferred to a combustion tube (quartz, 9 mm OD, 12 cm length) using 2 ml MQ water and speedvac-dried.

Structural C The extracted wood was washed twice with 10 ml MQ H_2O, dried at 60 °C and transferred to a disposable borosilicate glass culture tube (13 × 100 mm, VWR). Structural C was isolated from the remaining wood using the ABA method, a sequential extraction with acid (HCl), base (NaOH) and acid (HCl) followed by washing with MQ water (Gaudinski et al. 2005). However, we omitted the first acid extraction step of the ABA procedure because the samples had already been acid-extracted. This procedure yields (mostly) cellulose and lignin. Structural C samples were dried in the block heater at 60 °C. A subsample (2–4 mg) was transferred to a quartz combustion tube (15 cm length, 6 mm OD).

Radiocarbon analysis and reporting

The quartz tubes containing the three tree C fractions or bulk vegetation were evacuated, sealed and combusted at 900 °C for 2 h with 80 mg CuO. Sample CO_2, in quartz tubes and canisters, was isolated cryogenically, quantified manometrically on a vacuum line and reduced to graphite via zinc reduction (Xu et al. 2007, Graven et al. 2013). The NSC fractions are reported as NSC per gram of dry wood using the yield of CO_2, the relative volume of solution combusted to the total volume and mass of wood extracted.

Radiocarbon samples were analyzed with accelerator mass spectrometry (AMS) at the W. M. Keck Carbon Cycle AMS facility of UC Irvine (Southon et al. 2004, Southon and Santos 2007). Data are reported as fraction modern (FM), the ratio of the $^{14}C/^{12}C$ signature of the sample (corrected to $\delta^{13}C$ of –25‰) divided by that of an absolute ^{14}C standard (95% of the $^{14}C/^{12}C$ ratio of the oxalic acid I standard, corrected for radioactive decay of ^{14}C since 1950). With this notation, a FM = 1 indicates that the sample and standard have the same $^{14}C/^{12}C$ ratio (that of the pre-industrial atmospheric CO_2), values > 1 indicate the presence of 'bomb'-produced ^{14}C and values < 1 indicate that the time has been long enough for some radioactive decay to reduce $^{14}C/^{12}C$ ratios in the sample to below those of the pre-industrial atmospheric standard. It should be emphasized that the correction of reported ^{14}C data to a common $\delta^{13}C$ value means that any mass-dependent fractionation of the ^{14}C isotope is corrected out (assuming that the ^{14}C is fractionated twice as much as ^{13}C; see Stuiver and Polach 1977). Hence, the ^{14}C data reported here reflect differences in the time of fixation of CO_2 from the atmosphere or mixing of different-aged C pools.

Estimating C pool ages

Because we were unable to identify growth rings, despite repeated efforts, including wood staining, we used the ^{14}C 'bomb-spike' approach to estimate the mean age of C. The mean age represents the average time elapsed since original fixation of the C within NSC or structural pools (Gaudinski et al. 2001, Vieira et al. 2005, Carbone et al. 2013, Muhr et al. 2013, Richardson et al. 2013, 2015). In the mid-twentieth century, atmospheric thermonuclear weapons testing approximately doubled the ^{14}C content of CO_2 in the northern hemisphere

atmosphere. Since 1963, this 'bomb-^{14}C' has been declining in the atmosphere as CO_2 is exchanged with older C pools in oceans and soils and ^{14}C-free CO_2 is being emitted from fossil fuel burning (Levin et al. 2010). Structural C pools in a tree ring are predominantly formed from fresh photoassimilates or current CO_2 (Grootes et al. 1989, Gaudinski et al. 2005). During the bomb period, we can estimate the year a tree ring formed by comparing the ^{14}C content of the structural C pool with the record of northern hemisphere $^{14}CO_2$ (Figure 1).

We estimated the year of structural C formation, which represents the averaged time period over which a given stem core increment formed. As core increments were 2–4 cm in length, each one integrated 8–40 years of growth (Figure 1). We then calculated (i) the mean age of the NSC pools, as relative differences in the ^{14}C content of the structural C pool and the NSC pools within the same stem core increment can be expressed as differences in years and (ii) the rate of radial tree growth (formation year vs stem core increment).

For structural C formed between approximately 1650 and 1950, specific calendar years of wood formation cannot be estimated unambiguously from a comparison to the atmospheric $^{14}CO_2$ record (Cain and Suess 1976, Worbes 2002). We estimated the mean age of these 'pre-bomb' structural C pools by extrapolating radial growth rates from the post-bomb period (i.e., assuming that these are constant with time).

Model of NSC C transport and use in stems

We built a model to simulate the formation and subsequent mixing of NSC C through time (Figure 2). The model assumed that in every year (t), that year's photoassimilates, which have the same ^{14}C signature as that year's atmospheric CO_2, formed a fixed amount of immobile structural C and mobile NSC. In this model,

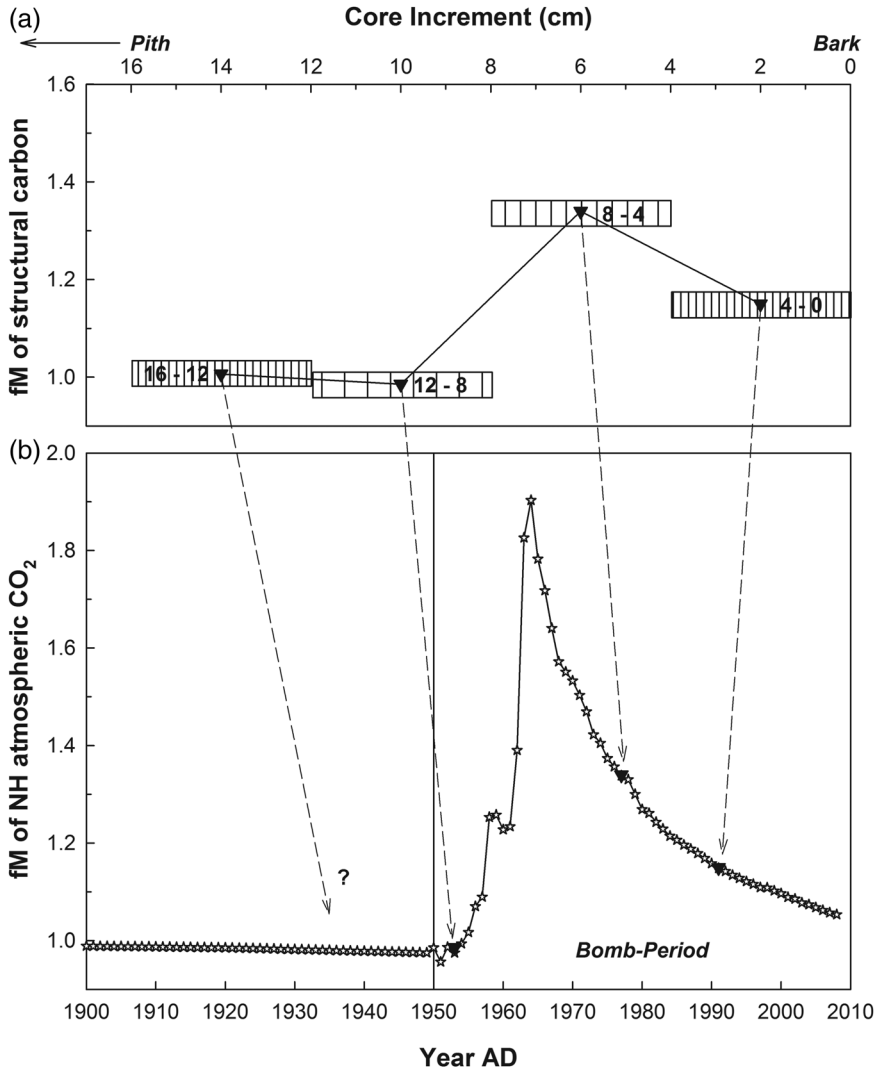

Figure 1. Illustration of the 'bomb-spike' approach: during the bomb period (1950 to present), the ^{14}C signature (expressed as FM) of a C pool formed predominantly from atmospheric CO_2 can be converted into one distinct calendar year. (a) Mean ^{14}C signature of the structural C pool of a tree as a function of sampling increment. Note that growth rate is not constant over time. (b) Mean annual ^{14}C signature of CO_2 in the northern hemisphere (NH) from 1900 to 2009 (1900–2007 (Levin et al. 2008), 2005–08 (I. Levin, personal communication)).

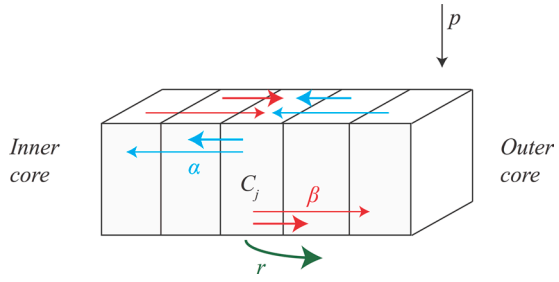

Figure 2. Schematic representation of our NSC-dynamics modeling approach for an arbitrary ring *j*. Each year a ring is formed and a constant amount *p* of new NSC enters the newest growth ring in the outer part of the core with the ^{14}C signature of the atmosphere for that year. Simultaneously, for all rings, a flux of NSC proportional to the mass of NSC in the ring leaves the system ($-kC_j$). A proportion of this lost NSC is transferred inward (α) or outward (β). This proportion decreases exponentially with the distance from the originating ring; i.e., α and β are not constant, but decline exponentially with distance according to the parameter γ. A proportion *r* (= 1 − α − β) of the lost NSC is not mixed into adjacent rings, but consumed and respired as CO_2. The flux of the respired CO_2 for any given ring (*j*) is $(1 - \Sigma_i\alpha_{ij} - \Sigma_i\beta_{ij})kC_j$. Movement in both directions occurs for all rings simultaneously, but is not presented explicitly for all rings due to space limitations. Additional details about the model are provided in Model of NSC C transport and use in stems.

we did not distinguish between 'soluble' and 'insoluble' pools (see Results). In years subsequent to formation, the amount and ^{14}C signature of the structural tissue remained constant, except for a very small loss due to radioactive decay over the century of simulation. The total amount of NSC lost from each ring was proportional to the amount stored in that ring that year. Loss can occur via two processes, mixing to other rings or respiration. A constant fraction of the NSC lost from each annual ring was allowed to mix with the neighboring rings in the inner and outer directions, with larger amounts of NSC moving to neighboring rings than to rings that are further away. The remaining fraction of the NSC lost each year was consumed by respiration and escaped as CO_2.

Mathematically, the model was defined as a set of differential equations, in which the amount of NSC (C_j) in the *j* ring ($j = 1, \ldots, n$) is represented as

$$\frac{dC_j(t)}{dt} = \sum_{j=1}^{n} \alpha_{i,j} kC_j(t) + \sum_{j=1}^{n} \beta_{i,j} kC_j(t) - kC_j(t) \quad (1)$$

where the coefficients $\alpha_{i,j}$ and $\beta_{i,j}$ represented the proportion of inputs to ring *j* from the outer or inner part of the core from ring *i*, respectively.

In the year of ring formation, inputs of NSC were from recent photoassimilates (*p*) and old NSC from the inner part of the core. Therefore, Eq. (1) was modified for the most recent (forming) ring

$$\frac{dC_j(t)}{dt} = p + \sum_{j=1}^{n} \beta_{i,j} kC_j(t) - kC_j(t) \quad (2)$$

More generally, the system of differential equations is expressed in the vector and matrix form

$$\frac{d\boldsymbol{C}(t)}{dt} = p \cdot \boldsymbol{I}(t) + \mathbf{A} \cdot \boldsymbol{C}(t) \quad (3)$$

where $\boldsymbol{C}(t)$ is a vector of length *n* containing the mass of NSC at time *t* and **A** is an $n \times n$ matrix containing the exit rate $-k$ in its diagonal and the transfer coefficients $\alpha_{i,j}$ and $\beta_{i,j}$ in the lower and upper diagonals, respectively. The components of the vector $\boldsymbol{I}(t)$ take the value 0 for all rings except the ring formed in the year *t*. More explicitly, $\boldsymbol{I}(t) = [I_1, \ldots, I_i, \ldots, I_n]^T$, where

$$I_i = \begin{cases} 1, & \text{if } i = t \\ 0, & \text{otherwise} \end{cases} \quad (4)$$

The movement of NSC to the inner and outer parts of the core was modeled using an exponential function that moved a larger amount of soluble C to the adjacent rings than to rings further away. Mathematically, this was represented as

$$\alpha_{i,j} = c_j \exp(-\gamma \cdot i) \quad (5)$$

$$\beta_{i,j} = d_j \exp(-\gamma \cdot i) \quad (6)$$

where c_j and d_j represented the total proportion of NSC transferred to the inner and outer parts of the core, respectively, and γ was the coefficient of exponential transfer. An important constraint on $\alpha_{i,j}$ and $\beta_{i,j}$ was that they must sum to the total proportions of inner and outer movement α and β, respectively. That is

$$\alpha = \sum_{i=j+1}^{n} c_j \exp(-\gamma i) \quad (7)$$

$$\beta = \sum_{i=j-1}^{1} d_j \exp(-\gamma i) \quad (8)$$

We therefore solved for c_j and d_j as

$$c_j = \frac{\alpha}{\sum_{i=j+1}^{n} \exp(-\gamma i)} \quad (9)$$

$$d_j = \frac{\beta}{\sum_{i=j-1}^{1} \exp(-\gamma i)} \quad (10)$$

The proportion of NSC that was not mixed with neighboring rings and consumed as respiration was calculated as

$$r = 1 - \alpha - \beta \quad (11)$$

The ^{14}C version of this model was mathematically identical, with the exception that the inputs of ^{14}C were based on the time history of ^{14}C of the atmospheric CO_2 $\mathrm{Atm}C^{14}(t)$, and radioactive decay was accounted for using the radioactive decay constant λ. Therefore,

$$\frac{d\boldsymbol{C}^{14}(t)}{dt} = p \cdot \boldsymbol{I}(t) \cdot \mathrm{Atm}C^{14}(t) + \boldsymbol{A} \cdot \boldsymbol{C}^{14}(t) - \lambda \cdot \boldsymbol{C}^{14}(t) \quad (12)$$

Eq. (12) was implemented in the R environment for computing using the SoilR package (Sierra et al. 2014).

We used Markov chain Monte Carlo (MCMC) to calculate values for k, α, β and γ from our largest available data set of NSC, those from the evergreen oak *Q. agrifolia*. We optimized the fit to trends between ring age (based on structural C) and the amount and ^{14}C signature of combined soluble and insoluble NSC. To have enough data points, we collated all the data from all *Q. agrifolia* trees, separated into two groups—slow- and fast-growing individuals (see Results). The method uses the delayed rejection and adaptive Metropolis procedure. As priors, we used the covariance matrix obtained by a preliminary optimization procedure using the Levenberg–Marquardt method. This method of combining traditional optimization and MCMC is described in Soetaert and Petzoldt (2010) and implemented in R within the package FME. We ran a total of 2500 chains and present as optimal parameters the mean ± standard deviation, and we minimized the difference in fit between the ^{14}C of soluble and structural C pools as well as required that the ^{14}C signature of the CO_2 produced by loss of soluble C be greater than observed in our measured stem CO_2 efflux. This modeling approach assumed that the measured CO_2 efflux contained contributions from both faster- and slower-cycling NSC pools (see Richardson et al. 2013, 2015), whereas our in-stem measurements emphasized the dynamics of the slow NSC pool. The model assumes no vertical transport of NSC in or out, as we had no data with which to constrain this flux.

Results

Evaluation of NSC extraction methods for C and ^{14}C analysis

Our methods for NSC extraction introduced small amounts of extraneous C to our samples. For soluble NSC, we processed a sucrose standard (ANU sucrose) in parallel with batches of core samples and compared the amount and ^{14}C signature of the processed samples with measurements of unprocessed standard material. We found that small amounts of extraneous C were added by our extraction procedure. The sucrose standard (expected to yield 420 mg C g^{-1} combusted based on stoichiometry) yielded 432.2 ± 22.4 (26) mg C g ANU^{-1}, compared with 466.3 ± 53.3 (14) mg C g ANU^{-1} (average ± SD (n)) following soluble NSC extraction. This is <10% of the measured soluble NSC values, and we have applied no correction to the data reported for soluble NSC here.

The consensus ^{14}C FM value of ANU sucrose (IAEA-C6) that is combusted, reduced to graphite and measured by AMS is 1.5025 ± 0.0004 (Xu et al. 2010). Initially, ANU processed as soluble NSC (methanol : H_2O extract) gave lower than expected ^{14}C values, which indicated the presence of a very small amount of ^{14}C-free C in the sample, likely methanol-C. Thus, we added wash steps (2× re-dissolution in MQ H_2O followed by speedvac drying) to the procedure (see Soluble NSC). The resulting FM of ANU processed as soluble NSC (1.4870 ± 0.0026, average ± SE, $n = 14$) was consistently reproducible but remained significantly lower (t-test $P < 0.001$) than the untreated ANU. Hence, our reported soluble extracts could be systematically low by 0.0155 FM, roughly four to five times our precision, or equivalent to a bias of up to 3 years too 'old' when we calculate the average age of this C, which is close to values for wood formed in the 1970s. We have not corrected for this potential bias in the data reported here, because it is small compared with the differences we report and interpret, especially given the number of years of growth represented in the 2–4 cm core sections. We conclude that methanol cannot be completely removed from the NSC fraction without drastically increasing the number of extraction steps and time, and thus risk of contamination with extraneous C. Data measured in our laboratory and reported in subsequent studies (Carbone et al. 2013, Richardson et al. 2013, 2015) used H_2O- rather than methanol : H_2O-based extraction and do not have similar drawbacks. Both extraction techniques include compounds other than simple sugars.

We created our own insoluble NSC standard because commercially available starch could not be recovered following our extraction methods. Thus, we analyzed frozen potatoes (Cascadian Farm French Fries, straight cut, which included organic potatoes, canola oil, apple juice and citric acid) alongside unknown samples. The ^{14}C signature of insoluble NSC isolated from this mixture with our extraction procedure was highly reproducible with a FM of 1.0520 ± 0.0016 (average ± SE, $n = 13$).

Suitability of the bomb-spike approach

At all four University of California reserves, the ^{14}C signature of annual plants equaled that of ^{14}C in well-mixed tropospheric CO_2 in the northern hemisphere (data presented with stem CO_2 efflux, discussed subsequently) during our measurement period (Levin et al. 2010). This indicates that the influence of local sources of ^{14}C-free CO_2 from fossil fuel combustion, ^{14}C-depleted CO_2 from ocean upwelling and of ^{14}C-enriched CO_2 as produced by waste incinerators and nuclear power plants were negligible, and we can apply the bomb-spike approach.

At Starr Ranch, annual plants and ambient CO_2 were depleted in their ^{14}C signature by local sources of ^{14}C-free CO_2. As both tree species measured at Starr Ranch experienced the same atmospheric variations, we can still compare the relative ^{14}C signatures of CO_2 exiting their stems, although absolute values will be affected by local uncertainties in atmospheric ^{14}C.

Oak tree growth rates

The ^{14}C signature of structural C indicated that cores from nearly all oak trees penetrated to wood that pre-dated the bomb period (1950+). Plotting of the average age (centroid year) of each post-bomb core segment vs core depth yielded an estimate of the mean radial growth rate of these trees. Growth rates ranged

from 0.04 to 0.6 cm year^{-1} and were faster at the more southern locations of each species (see Table S1 available as Supplementary Data at *Tree Physiology* Online). The fastest growth rates were observed for *Q. agrifolia*, which grew three times faster at the two more southern sites than at the two more northern sites (Figure 3 and Table 2, showing data for *Q. agrifolia* only). For all trees in which we had enough post-bomb points to extrapolate a growth rate, we extrapolated this relationship (using the slopes from Table 2 or S1 available as Supplementary Data at *Tree Physiology* Online, depending on species) to estimate the approximate years of growth for core sections with ^{14}C ages, indicating that they were formed in the 1560–1950 period. These estimated ages were used for plotting pre-bomb points in time in subsequent figures.

Non-structural carbon concentration

In *Q. agrifolia* and *Q. lobata*, concentrations of both NSC fractions were highly variable, and there was no trend in the NSC concentration as a function of the mean age (depth) of the core segment (see Figure S2 available as Supplementary Data at *Tree Physiology* Online). Across all species, and averaged over the whole core length, more soluble NSC was extracted (expressed per milligram of dry wood) compared with insoluble NSC (Figure 4). Within our limited data set, there were no obvious differences in soluble NSC concentrations between species or locations, but *Q. agrifolia* had consistently the highest concentrations of insoluble NSC (Figure 4). For *Q. agrifolia* (the species for which we have the most data), we could resolve no seasonal trend in NSC abundance (Table 2).

Radiocarbon signatures of NSC

In all oak species, soluble and insoluble fractions had ^{14}C signatures, indicating that NSC is younger than the structural material from which it was extracted (Figures 5 and S3 available as Supplementary Data at *Tree Physiology* Online). During the bomb period, this means that the ^{14}C signatures of soluble and insoluble

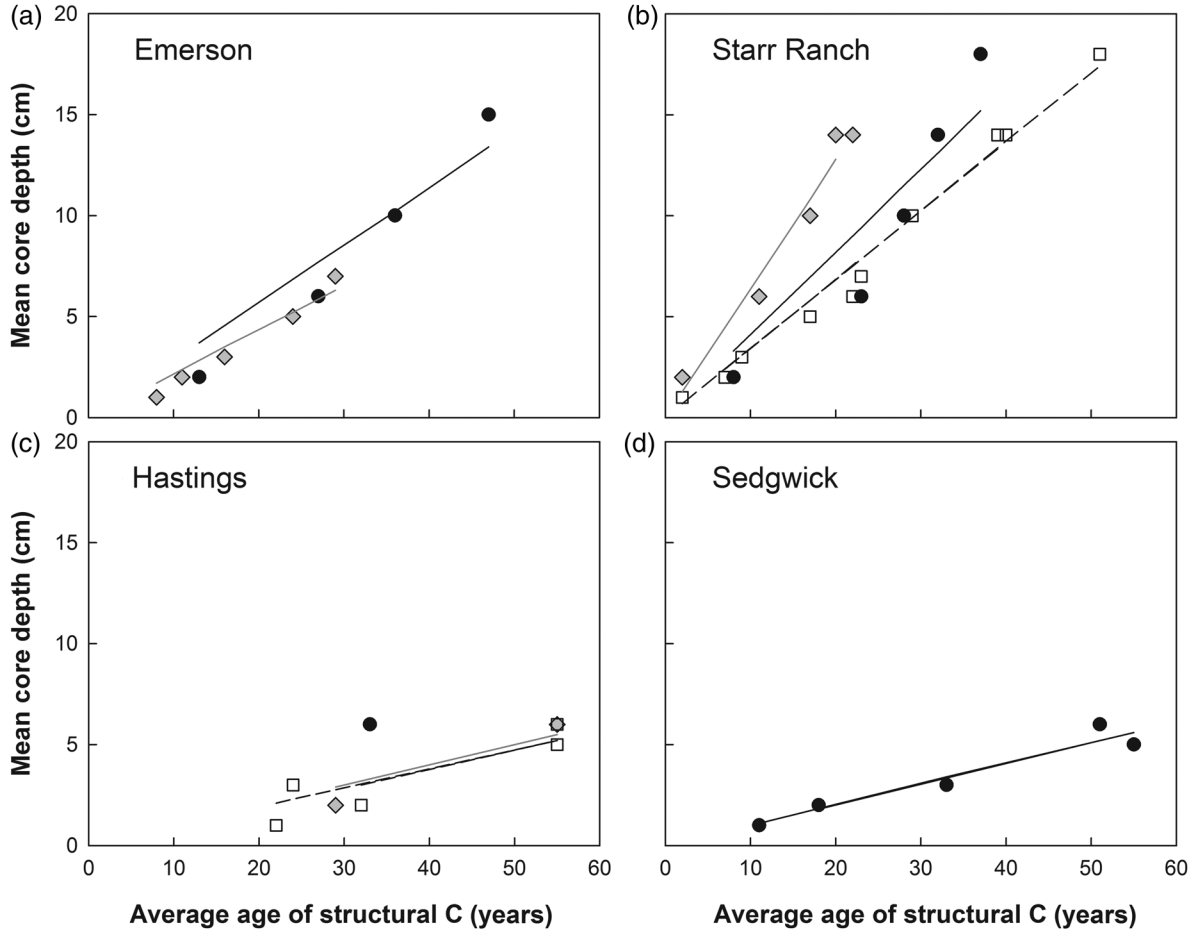

Figure 3. Relationship between depth in a tree core (0 cm = outermost wood) and the age of structural C (in years before the year of sampling, 2008) for *Q. agrifolia*. Ages were estimated by comparing the ^{14}C signature of the structural C with the time history of atmospheric $^{14}CO_2$ during the bomb period. The slopes provide a measure of the relative radial growth rates for these trees and demonstrate faster growth at the two southernmost sites (Emerson and Starr Ranch) compared with the northern sites (Hastings and Sedgwick). (Each symbol and line type represents an individual tree. Slope parameters are given in Table 2.)

Table 2. Estimated growth rates (slope in cm core increment per year) using least-squares method (Figure 3) and mean concentrations (mg C (g wood)$^{-1}$) of soluble and insoluble NSC for *Q. agrifolia* only. Each row presents data from a single tree. In some cases, points from two (or in one case three) cores from the same tree were combined to estimate the linear regressions. Data for other species are given in Table S1 available as Supplementary Data at *Tree Physiology* Online. n.a., not applicable ($n = 1$); n.m., not measured.

	No. of cores/ tree[1]	Slope	R^2	Soluble NSC				Insoluble NSC	
				Winter		Summer		Annual	
				Mean (SD)	*n*	Mean (SD)	*n*	Mean (SD)	*n*
Sedgwick	2 (5)	0.1015	0.98	46.7 (10.3)	4	32.9* (7.3)	4	14.4 (12.1)	8
Hastings	1 (1)	0.1818	n.a.	17.1 (n.a.)	1	n.m.	0	0.7 (n.a.)	1
	1 (2)	0.1004	0.97	36.4 (0.7)	2	n.m.	0	17.7 (11.3)	2
	2 (5)	0.0938	0.95	35.8 (15.3)	4	25.8* (5.3)	4	8.6 (5.9)	7
Starr Ranch	1 (5)	0.4106	0.96	20.6 (1.0)	5	n.m.	0	n.m.	0
	2 (5)	0.6379	0.99	24.5 (8.7)	8	n.m.	0	3.6 (3.7)	7
	3 (11)	0.3416	0.99	24.1 (12.1)	7	28.3* (3.2)	4	3.4 (3.2)	11
Emerson	1 (4)	0.2846	0.98	33.2 (9.4)	4	n.m.	0	12.9 (8.3)	4
	2 (5)	0.2158	0.98	n.m.	0	30.1 (3.4)	4	7.4 (n.a.)	1

[1]Number of post-bomb ^{14}C measurements used to calculate the growth rates; the year of sampling (2008 = 0 cm) was used as an additional constraint.

*Summer and winter concentrations are significantly different ($P < 0.5$; unpaired Student's *t*-test).

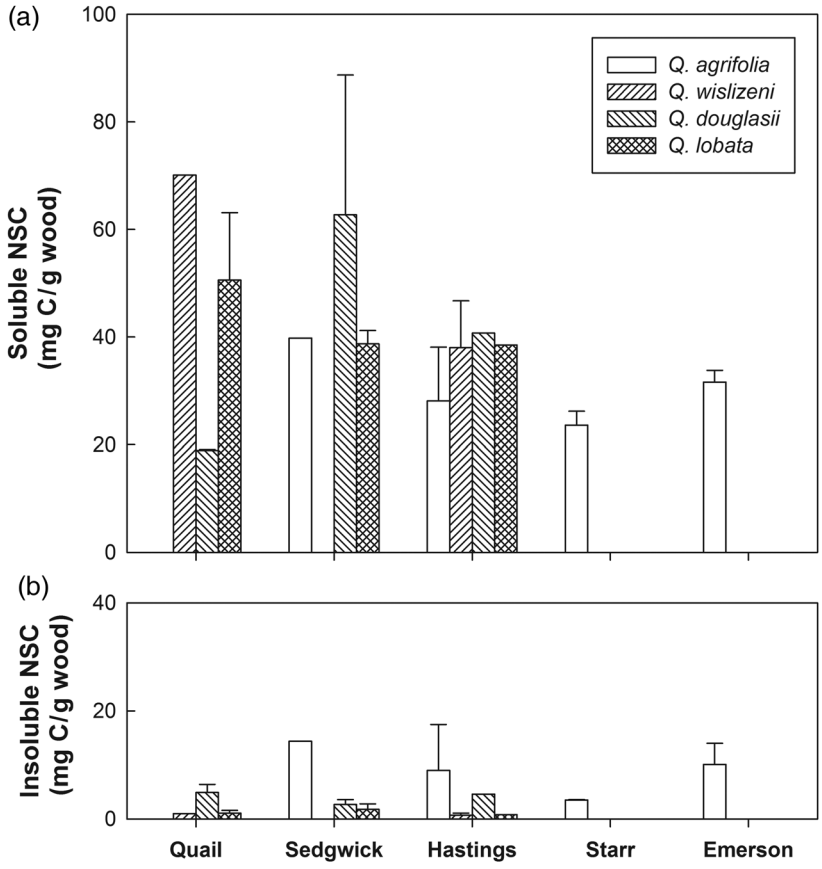

Figure 4. Average concentration of (a) soluble and (b) insoluble NSC in California oaks (average ± SD, $n = 1$–4 trees).

NSC were lower than those of the extracted structural material. For wood formed before the bomb peak, both soluble and insoluble NSC contained bomb-derived C, extending back up to several hundred years in slower-growing trees. These patterns were similar for all species (only *Q. agrifolia* and *Q. lobata*, the species for which we were able to obtain data from several individuals, are shown in Figure 5; other species are shown in Figure S4 available as Supplementary Data at *Tree Physiology* Online). Radiocarbon data obtained from different tree cores of the same *Q. agrifolia* individuals were highly reproducible (within AMS

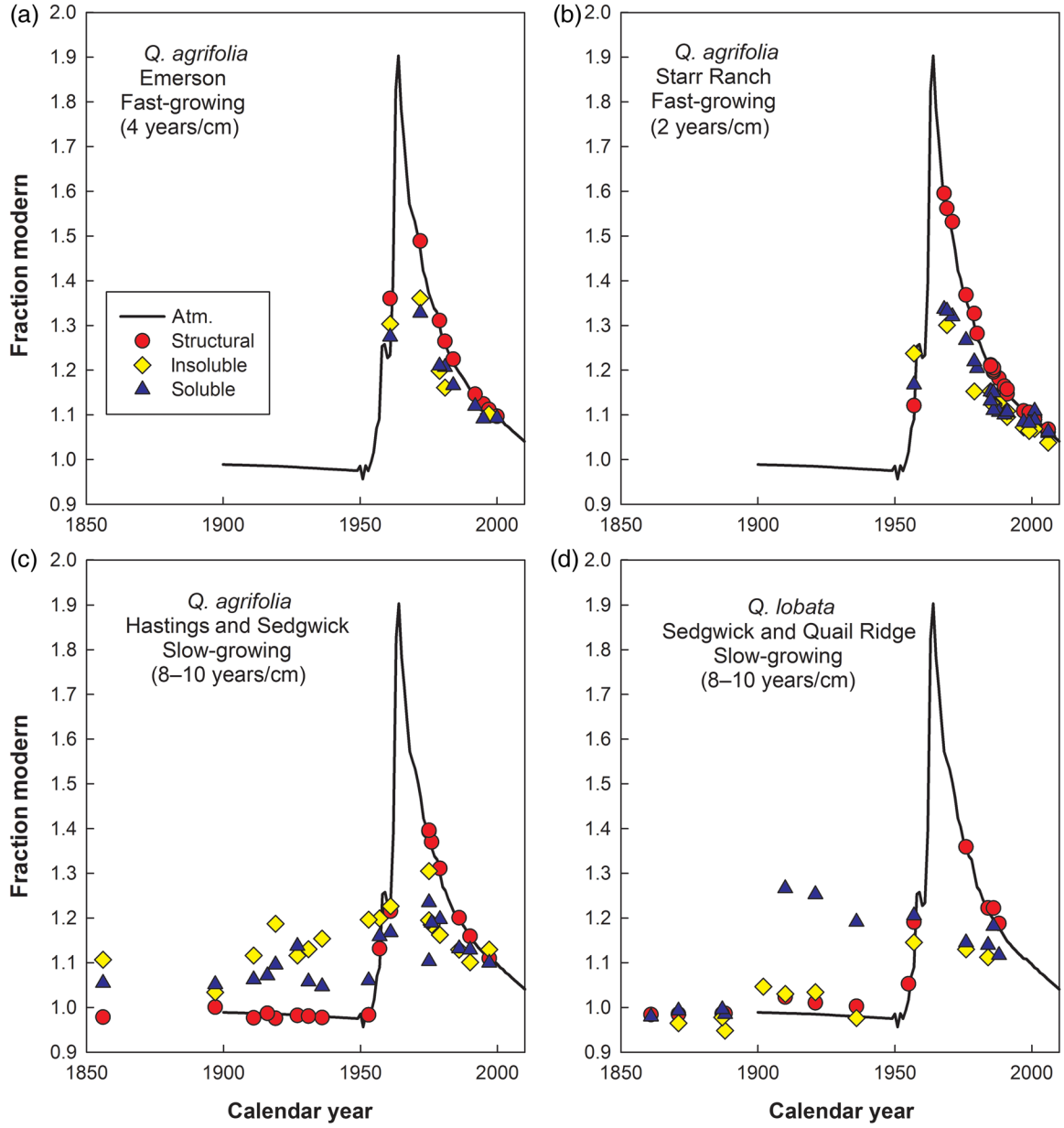

Figure 5. Radiocarbon in structural C (circles), plotted on the atmospheric record (line) to identify average time when it was fixed from the atmosphere (Figure 1). The ^{14}C signatures of soluble (triangle) and insoluble (diamond) fractions are plotted on the same time scale (i.e., for comparing the age of ^{14}C with that of the structural C from which it was extracted). Data shown are for the two sites with faster-growing *Q. agrifolia* (top) and combine two sites each with slower-growing *Q. agrifolia* (bottom left) and *Q. lobata* (bottom right). Data for other trees are shown in Figure S4 available as Supplementary Data at *Tree Physiology* Online.

measurement uncertainty). Given the large differences in growth rates within a species (Figure 3), and with few data available in the post-bomb period for many of the slower-growing trees we sampled, we could not identify any obvious differences in patterns between deciduous (*Q. lobata*) and evergreen (*Q. agrifolia*) oak species.

The ^{14}C signatures of soluble and insoluble NSC fractions extracted from the same core segment mostly fell within 0.05 FM of the 1 : 1 line (dashed line in Figure 6). For species other than *Q. agrifolia*, insoluble NSC in some cases had lower ^{14}C than soluble C extracted from core segments that integrate the time period closest to the bomb peak, when ^{14}C changes in the atmosphere were most rapid and pronounced. Because the insoluble fraction represented a relatively minor amount of C compared with the soluble fractions, we used only the soluble fraction as the 'mobile' pool in our subsequent modeling.

Carbon dioxide efflux from tree stems

The rate of CO_2 efflux from oak (but not the sycamore) stems was greatest just after chamber installation, likely a consequence of removing the cork (see Figure S5 available as Supplementary Data at *Tree Physiology* Online). Later, CO_2 efflux rates ranged

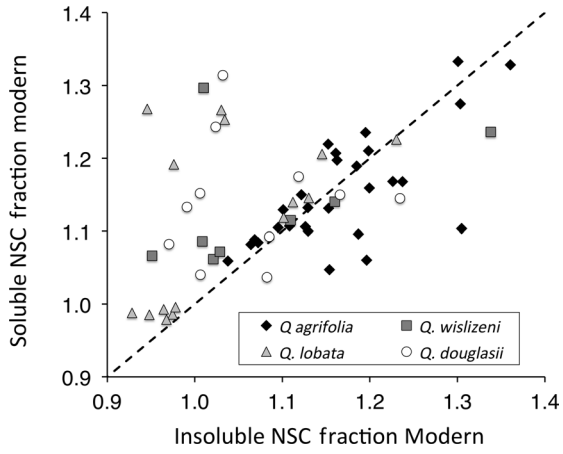

Figure 6. Comparison of the ^{14}C signatures (in FM) of insoluble and soluble NSC extracted from the same piece of core for the four oak species across all sites we studied. The 1 : 1 line is shown as the dashed line; most points fall within 0.05 FM.

from 1 to 5 μmol C m^{-2} s^{-1}, with higher fluxes observed for the evergreen oak (*Q. agrifolia*) than the deciduous species (*Q. lobata*, *Q. douglasii*, *Q. lobata*, *P. racemosa*). Growth rates (Figure 3) were higher in *Q. agrifolia* at Starr Ranch compared with Sedgewick, whereas CO_2 efflux was higher for this species at Sedgewick (see Figure S5 available as Supplementary Data at *Tree Physiology* Online).

Radiocarbon of tree CO_2 efflux

The ^{14}C signature of CO_2 emitted from all tree stems was enriched relative to the ^{14}C signature of photoassimilates (ambient CO_2) and more enriched in the evergreen than in the deciduous species (Figure 7). At Sedgwick, the CO_2 emitted by evergreen oaks (*Q. agrifolia*) was enriched by 0.015–0.020 FM, which was larger than the analytical error associated with collection and analysis of CO_2 samples using pre-evacuated canisters (0.002–0.003 FM (Graven et al. 2013)). The ^{14}C signature of

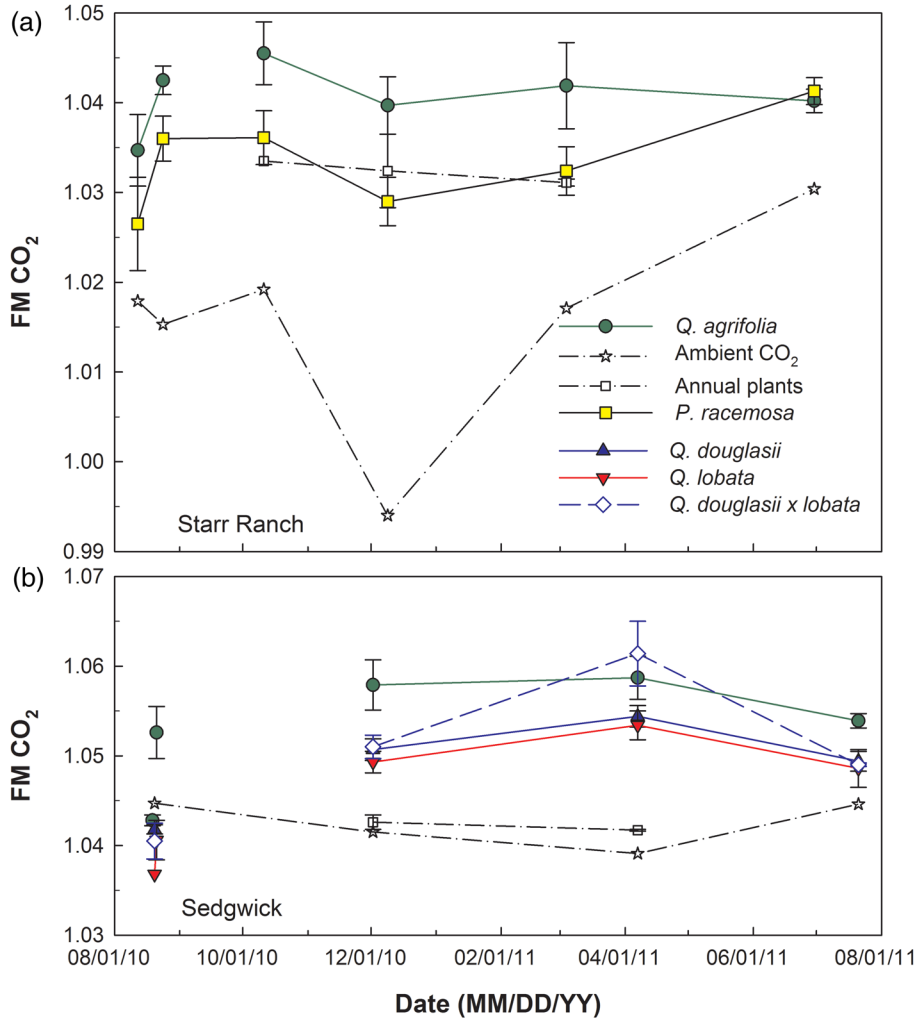

Figure 7. Seasonal pattern of the ^{14}C signature (expressed as FM) of CO_2 efflux from tree stems of evergreen (*Q. agrifolia*) and deciduous oaks (*Q. douglasii*, *Q. lobata*) and sycamore (*P. racemosa*) (average ± SE, $n = 2–5$), of CO_2 in ambient air ($n = 1$) and of bulk annual plant leaves (average ± SE, $n = 2$). At (a) Starr Ranch, *P. racemosa* had no green foliage on 11 October and 9 December 2010. At (b) Sedgwick, *Q. douglasii* and *Q. lobata* had no green foliage on 2 December 2011.

CO_2 emitted from the deciduous oaks was less enriched (0.010–0.015 FM), with highest values observed right after leaf flushing (7 April 2011). The results from Sedgwick indicate that the C source of CO_2 emissions was on average 2–4-year-old C in the evergreen oaks and 1–2-year-old C for the deciduous oaks.

Rates of mixing vs loss of NSC derived from modeling depth profiles

To constrain parameter estimation, we combined the data for soluble NSC from all cores of *Q. agrifolia* (the species with most analyses). Because it proved difficult to constrain the model with all data together, we separated the data into two groups: sites with faster- (Emerson and Starr Ranch) vs slower-growing trees (Sedgewick and Hastings; Figures 3 and 5). Those data are shown together with the best fits obtained from the Bayesian analysis (Figure 8 and Table 3). An additional constraint for the model was the requirement to maintain constant NSC concentrations with depth in the stem (see Figure S2 available as Supplementary Data at *Tree Physiology* Online).

The proportion of NSC consumed by respiration ($r = 1 - \alpha - \beta$; Eq. (11)), and not mixed with neighboring rings, was larger in faster-growing trees ($r = 0.397 \pm 0.260$) than in slower-growing trees ($r = 0.034 \pm 0.047$) (Table 3). The rate of NSC consumption, calculated as $k \times r$, was 0.157 ± 0.105 year^{-1} for faster-growing trees (average turnover time of 6 years, with standard deviation 4–19 years) and 0.017 ± 0.022 year^{-1} for slower-growing trees (average turnover time of 59 years, with standard deviation >26 years). Results for slower-growing trees were highly uncertain given the need to estimate the ages of wood core increments during the pre-bomb era from very limited information on post-1963 growth rates and the lack of constraint in the most recent decade (because a 2 cm increment already averages nearly two decades in slower-growing trees). Notably, the values of k (Table 3) were similar for both faster- and slower-growing trees, but the models suggested that respiration is more important than mixing in faster-growing trees, whereas mixing was more important in slower-growing trees.

The model was also used to calculate the stem balance of NSC by comparing the amount of C added in 2010 to the outermost ring with the integrated loss of C through respiration across all rings in the same year. For the best-fit run, only 22% of the added C was respired in the slower-growing trees, but 92% in the faster-growing trees. By summing the amount of C respired together with its ^{14}C content across all rings, we estimated the FM for respired CO_2 from the stem in 2010. This was 1.145 FM for slower-growing trees and 1.090 FM for faster-growing trees. Observed *Q. agrifolia* CO_2 efflux measured with

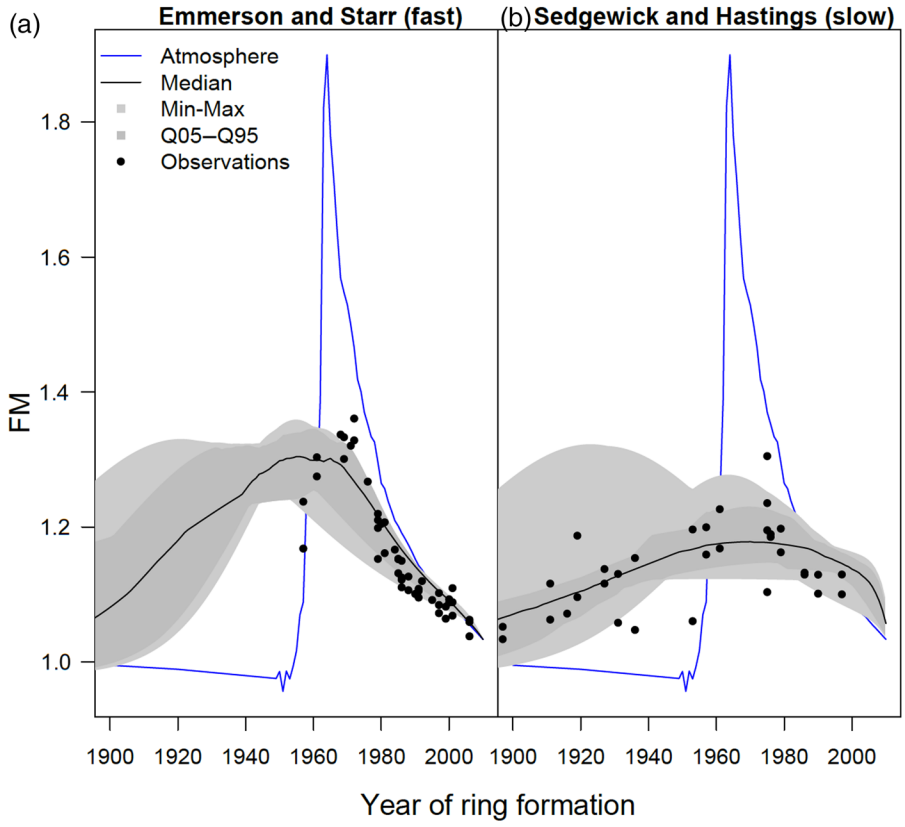

Figure 8. Model fits to ^{14}C signature (expressed as FM) in soluble NSC fractions for *Q. agrifolia* from (a) faster-growing trees (Emerson and Starr Ranch) compared with (b) slower-growing trees (Sedgewick and Hastings) that have fewer constraints in the post-bomb period. Best-fit parameters are given in Table 3.

Table 3. Summary statistics of the fitted parameters for *Q. agrifolia* growing faster at Emerson and Starr Ranch and slower at Sedgewick and Hastings sampling sites. The parameters are defined as follows: k is the rate at which soluble NSC leaves a tree ring every year; α and β are dimensionless and represent the proportion of NSC that leaves each ring and provides inputs to other rings, α from the outer toward inner and β from the inner toward outer parts of the stem, respectively; γ is the coefficient of exponential transfer of NSC from each ring. Additional details about the parameters are found in Model of NSC C transport and use in stems and Figure 2.

	k (year^{-1})	α	β	γ	r	$k \times r$
Faster-growing trees						
Mean	0.320	0.236	0.366	0.306	0.397	0.157
SD	0.037	0.259	0.051	0.025	0.260	0.105
Min	0.261	0.008	0.245	0.227	0.001	0.001
Max	0.501	0.995	0.489	0.349	0.725	0.314
Q0.25	0.357	0.027	0.349	0.288	0.267	0.096
Q0.50	0.390	0.158	0.356	0.312	0.421	0.152
Q0.75	0.398	0.336	0.399	0.322	0.623	0.248
Slower-growing trees						
Mean	0.434	0.418	0.548	0.127	0.034	0.017
SD	0.170	0.126	0.117	0.055	0.046	0.022
Min	0.051	0.139	0.303	0.019	0.001	0.001
Max	0.774	0.710	0.866	0.271	0.291	0.146
Q0.25	0.394	0.352	0.506	0.093	0.014	0.007
Q0.50	0.448	0.402	0.549	0.125	0.027	0.013
Q0.75	0.516	0.454	0.587	0.162	0.043	0.021

chambers (Figure 7) averaged lower than these values, about 1.040 FM for Starr Ranch (fast-growing) and 1.055–1.060 for Sedgwick Ranch (slow-growing).

Discussion

Importance of lateral mixing of NSC in tree stems

Our results confirm a number of recently published studies, indicating that NSC reserves in tree stems can be decades old (Richardson et al. 2013, 2015) and that these old reserves are used to maintain respiration (Carbone et al. 2013, Muhr et al. 2013). As found by Richardson et al. (2013) using similar methods, soluble and insoluble NSC fractions have similar ^{14}C signatures (Figure 6), suggesting that they interchange rapidly compared with the rates of lateral mixing. Our results extend these studies to show that NSC continues to get older the deeper in tree stems it is. We also clearly demonstrate that older C pools, with ages that are consistent with the NSC pools found in the wood, actively contribute year-round to the CO_2 efflux from stems of evergreen oaks in CA (Figure 7). These results add to those found for mature temperate (Carbone et al. 2013) and tropical forest trees (Muhr et al. 2013).

Hoch et al. (2003) observed that NSC concentrations in *Q. petraea* declined with sapwood depth and reached a stable minimum in the heartwood. The constant amount of soluble and non-soluble NSC in our oak stemwood, regardless of depth (see Figure S2 available as Supplementary Data at *Tree Physiology* Online), was, however, consistent with other studies, demonstrating that NSC dynamics are highly variable among species (Hoch et al. 2003, Würth et al. 2005).

The ^{14}C signature indicated that the C in NSC was fixed after the structural C at the same depth in the stem, providing incontrovertible evidence that NSC concentrations deeper in the stem are partly maintained by inward mixing of younger NSC. The model we applied fits the dual requirements of constant NSC with depth by rapid lateral mixing that replaces C lost by respiration in both slower- and faster-growing trees. As noted earlier, our one-dimensional approach ignores potential vertical fluxes.

Mediterranean oaks such as *Q. agrifolia* have prominent ray parenchyma as well as hard-to-distinguish annual rings (Snow 1903). Future studies should link NSC lateral movement and use in stems to wood anatomy, in particular, parenchyma structure (Plavcová and Jansen 2015).

NSC dynamics and use with climate and leaf habit

Contrary to our initial hypothesis, we did not observe large differences in the age or depth distribution of NSC with climate (decreasing MAP). Drought has been shown to deplete NSC in roots, but not needles or branches, when photosynthesis and NSC translocation become impaired (Hartmann et al. 2013*a*, 2013*b*, 2015, Klein et al. 2014). Here, the similar NSC dynamics between sites imply that within their natural range, trees compensated for changes in environmental conditions, including precipitation. Growth conditions reflect the complex interactions among (highly variable) water-year precipitation, growing season temperature, access to groundwater (and possibly fog), soil conditions, elevation, aspect and land-use history (Pavlik et al. 2006, Abatzoglou et al. 2009).

We also did not observe large differences in the age or depth distribution of NSC between evergreen and deciduous oaks, suggesting that NSC dynamics in trees, in general, might be modeled irrespective of leaf habit and species, such as evergreen vs deciduous hardwoods (this study) or evergreen softwoods vs deciduous hardwoods (Richardson et al. 2015). The NSC pool size and rate of inward mixing of younger NSC, however, may vary with life traits. Richardson et al. (2015) observed stronger mixing-in in a temperate, evergreen softwood (*Pinus strobus* L.) compared with a hardwood (*Quercus rubra* L.). Differences in NSC dynamics can also be expected with water regulation (more efficient allocation of NSC in anisohydric trees (McDowell et al. 2008, Hartmann et al. 2013*a*)) and 'vigor' (faster-growing trees have larger and younger NSC pools (Carbone et al. 2013)) and possibly disturbance ecology (i.e., the ability to re-sprout).

Here, we found that growth rates of the trees varied considerably from one site and species to another and that this difference had the largest effect on the results we obtained. Overall, it was interesting that inward mixing rates apparently tended to scale with growth rates in these trees, given the similarity of the

distribution of ^{14}C with depth in the stems in all oak species we sampled (Figures 5 and S3 and S4 available as Supplementary Data at *Tree Physiology* Online).

We observed a strong control of growth rate on NSC usage. Within the single evergreen species *Q. agrifolia*, the models that reproduced the ^{14}C signature of NSC suggested that faster-growing trees respired a larger proportion and stored (by inward mixing) less of their NSC. These faster-growing trees may also produce a larger amount of NSC every year to compensate for larger losses in comparison with the slower-growing trees. We observed that the ^{14}C signature of CO_2 efflux from slower-growing *Q. agrifolia* at Sedgewick reserve, when compared with recent photoassimilates (annual plants), was higher compared with Starr Ranch (faster-growing) (Figure 7). Our model also predicted this difference, although predictions, particularly for slower-growing trees, were highly uncertain.

We also observed differences in the age of stem CO_2 efflux that may reflect leaf habit differences in the use vs storage of NSC. At the Sedgewick site, we sampled stem CO_2 efflux from deciduous and evergreen trees with similar (slow) growth rates. In the deciduous oaks, older NSC reserves contributed to a lesser degree to the stem CO_2 efflux than in evergreen oaks and only during the dormant and early growing season, but not during the late growing season.

Overall, our results corroborated the limited usage of older, stored NSC in a deciduous, temperate tree (*Acer rubrum* L.) (Carbone et al. 2013). Although it was clear that stem CO_2 efflux did not necessarily represent solely the production of C underneath the stem chamber, we assumed that the older NSC inside stems must contribute to the enhanced ^{14}C signature of the stem CO_2 efflux. It is reasonable, as found in Muhr et al. (2013), that the in-stem CO_2 was higher in ^{14}C signature than what is emitted from the stem surface. A better constraint could be provided by sampling in-stem CO_2 (Muhr et al. 2013) or by incubating stem cores to measure locally respired CO_2 directly.

Unlike the model of Richardson et al. (2013), we attempted to reproduce the conditions for inward mixing of younger, soluble NSC phases; hence, we did not de facto distinguish a 'fast' and 'slow' cycling pool for NSC, but assumed only a single NSC pool that persists in stems over years to decades of tree growth and results from the mixing of photoassimilates of different ages. Although the mean turnover times of this pool estimated by the model for faster-growing trees (average 6 years, 95% confidence interval (CI) = 4–19 years) were much shorter than those of the slower-growing trees (average 59 years, 95% CI >25 years), the associated uncertainties were large. Because we saw no large decline in soluble and insoluble NSC with depth in the core, the rate of NSC consumption (k) cannot be large for these NSC pools to persist over long periods of decades. If we assumed equal amounts of initial NSC allocation to new stemwood, the amount of C in the interior predicted from our 'faster' model would be very low compared with that predicted from the 'slower' model. However, we did not measure such large differences in the extractable NSC amounts between faster- and slower-growing trees. We also did not see large season differences in the NSC, probably because in slow-growing oaks even the outermost samples integrated many years of growth.

Although the models we used were able to successfully simulate the multiple observational constraints of constancy of NSC concentration with depth in the stem, lateral mixing resulting in younger NSC migrating inward in the stems and respired CO_2 with values higher than recent photoassimilates, the models have very large uncertainties, particularly for slower-growing trees. A major problem with the oaks we sampled was that growth rates in some trees were so slow that the 2 cm core sample needed to obtain sufficient extractable NSC for ^{14}C analysis integrated 15–20 years of structural C. The model also ignores vertical transport of NSC, which undoubtedly also occurs in tree stems. To improve our understanding of the role of mixing and utilization of NSC in tree stems, we recommend sampling in trees with visible rings and by ring or known number of rings as in Carbone et al. (2013) and Richardson et al. (2013, 2015).

Conclusion

We measured and modeled the NSC pool size, dynamics and allocation in five Mediterranean tree species. We found that across a natural species' range, not climate, but 'vigor' (growth rate) largely controlled the size, age and allocation of NSC pool to storage and respiration, with faster-growing trees respiring more and storing (by inward mixing) less of their NSC. Leaf habit also impacted NSC allocation as older NSC contributed more to stem CO_2 emissions in evergreen than in deciduous trees.

Our data corroborated that mature trees accumulate years-to-decade-old NSC across a wide climatic range (tropical, Mediterranean and temperate) to fuel respiration and recovery. Further advancing our understanding of the role of NSC in forest resilience to changing disturbance regimes, climate and rising atmospheric CO_2 requires combining observations of NSC dynamics, water status and wood anatomy and tree C uptake and loss, investigating whole-tree NSC dynamics (stem, branches and roots), ^{14}C analysis of single NSC compounds and bringing ecosystem ecologists together with molecular plant physiologists.

Supplementary data

Supplementary data for this article are available at *Tree Physiology* Online.

Acknowledgments

We thank K. Druffel-Rodriguez, A. Stills, E. Salamanca, M. Lupascu, P. Gao and A. Abbasi (UC Irvine) and M. Carbone (US

National Center for Ecological Analysis and Synthesis) for their assistance in the field and/or laboratory. We are grateful to the manager of the University of CA Sedgwick Reserve (K. McCurdy) and the director of the CA Audubon Starr Ranch Sanctuary (S. DeSimone) for their support of our research activities, granting access to the field sites and logistical support.

Conflict of interest

None declared.

Funding

This work was funded by the US National Science Foundation (IOS-0726332 to C.I.C. and S.T.).

References

Abatzoglou JT, Redmond KT, Edwards LM (2009) Classification of regional climate variability in the state of California. J Appl Meteorol Climatol 48:1527–1541.

Barbaroux C, Breda N (2002) Contrasting distribution and seasonal dynamics of carbohydrate reserves in stem wood of adult ring-porous sessile oak and diffuse-porous beech trees. Tree Physiol 22: 1201–1210.

Barbaroux C, Breda N, Dufrêne E (2003) Distribution of above-ground and below-ground carbohydrate reserves in adult trees of two contrasting broad-leaved species (*Quercus petraea* and *Fagus sylvatica*). New Phytol 157:605–615.

Cain WF, Suess HE (1976) Carbon 14 in tree rings. J Geophys Res 81:3688–3694.

Carbone M, Trumbore S (2007) Contribution of new photosynthetic assimilates to respiration by perennial grasses and shrubs: residence times and allocation patterns. New Phytol 176:124–135.

Carbone MS, Czimczik CI, McDuffee KE, Trumbore SE (2007) Allocation and residence time of photosynthetic products in a boreal forest using a low-level ^{14}C pulse-chase labeling technique. Glob Change Biol 13:466–477.

Carbone MS, Czimczik CI, Keenan TF, Murakami PF, Pederson N, Schaberg PG, Xu X, Richardson AD (2013) Age, allocation and availability of nonstructural carbon in mature red maple trees. New Phytol 200:1145–1155.

Chapin FS, Schulze E, Mooney HA (1990) The ecology and economics of storage in plants. Annu Rev Ecol Syst 21:423–447.

Czimczik CI, Trumbore SE, Carbone MS, Winston GC (2006) Changing sources of soil respiration with time since fire in a boreal forest. Glob Change Biol 12:957–971.

Dietze MC, Sala A, Carbone MS, Czimczik CI, Mantooth JA, Richardson AD, Vargas R (2014) Nonstructural carbon in woody plants. Annu Rev Plant Biol 65:667–687.

Ericsson T, Rytter L, Vapaavuori E (1996) Physiology of carbon allocation in trees. Biomass Bioenerg 11:115–127.

Gaudinski J, Trumbore S, Davidson E, Cook A, Markewitz D, Richter D (2001) The age of fine-root carbon in three forests of the eastern United States measured by radiocarbon. Oecologia 129:420–429.

Gaudinski JB, Dawson TE, Quideau S, Schuur EAG, Roden JS, Trumbore SE, Sandquist DR, Oh S-W, Wasylishen RE (2005) Comparative analysis of cellulose preparation techniques for use with ^{13}C, ^{14}C, and ^{18}O isotopic measurements. Anal Chem 77:7212–7224.

Gaudinski JB, Torn MS, Riley WJ, Swanston C, Trumbore SE, Joslin JD, Majdi H, Dawson TE, Hanson PJ (2009) Use of stored carbon reserves in growth of temperate tree roots and leaf buds: analyses using radiocarbon measurements and modeling. Glob Change Biol 15:992–1014.

Gholz HL, Cropper WP Jr (1991) Carbohydrate dynamics in mature *Pinus elliottii* var. *elliottii* trees. Can J For Res 21:1742–1747.

Gomez L, Bancel D, Rubio E, Vercambre G (2007) The microplate reader: an efficient tool for the separate enzymatic analysis of sugars in plant tissues—validation of a micro-method. J Sci Food Agric 87:1893–1905.

Graven H, Xu X, Guilderson TP, Keeling RF, Trumbore SE, Tyler S (2013) Comparison of independent delta $^{14}CO_2$ records at point barrow, Alaska. Radiocarbon 55:1541–1546.

Grootes PM, Farwell GW, Schmidt FH, Leach DD, Stuiver M (1989) Rapid response of tree cellulose radiocarbon content to changes in atmospheric $^{14}CO_2$ concentration. Tellus B 41:134–148.

Grulke NE, Andersen CP, Hogsett WE (2001) Seasonal changes in above- and belowground carbohydrate concentrations of ponderosa pine along a pollution gradient. Tree Physiol 21:173–181.

Hartmann H, Ziegler W, Trumbore S (2013*a*) Lethal drought leads to reduction in nonstructural carbohydrates in Norway spruce tree roots but not in the canopy. Funct Ecol 27:413–427.

Hartmann H, Ziegler W, Kolle O, Trumbore S (2013*b*) Thirst beats hunger—declining hydration during drought prevents carbon starvation in Norway spruce saplings. New Phytol 200:340–349.

Hartmann H, McDowell NG, Trumbore S (2015) Allocation to carbon storage pools in Norway spruce saplings under drought and low CO_2. Tree Physiol 35:243–252.

Hoch G, Körner C (2003) The carbon charging of pines at the climatic treeline: a global comparison. Oecologia 135:10–21.

Hoch G, Richter A, Körner C (2003) Non-structural carbon compounds in temperate forest trees. Plant Cell Environ 26:1067–1081.

Keel SG, Siegwolf RTW, Jäggi M, Körner C (2007) Rapid mixing between old and new carbon pools in the canopy of mature forest trees. Plant Cell Environ 30:963–972.

Klein T, Hoch G, Yakir D, Körner C (2014) Drought stress, growth and nonstructural carbohydrate dynamics of pine trees in a semi-arid forest. Tree Physiol 34:981–992.

Körner C (2003) Carbon limitation in trees. J Ecol 91:4–17.

Kozlowski TT (1992) Carbohydrate sources and sinks in woody plants. Bot Rev 58:107–222.

Kuptz D, Fleischmann F, Matyssek R, Grams TEE (2011) Seasonal patterns of carbon allocation to respiratory pools in 60-yr-old deciduous (*Fagus sylvatica*) and evergreen (*Picea abies*) trees assessed via whole-tree stable carbon isotope labeling. New Phytol 191:160–172.

Langley J, Drake B, Hungate B (2002) Extensive belowground carbon storage supports roots and mycorrhizae in regenerating scrub oaks. Oecologia 131:542–548.

Levin I, Hammer S, Kromer B, Meinhardt F (2008) Radiocarbon observations in atmospheric CO_2: determining fossil fuel CO_2 over Europe using Jungfraujoch observations as background. Sci Total Environ 391:211–216.

Levin I, Naegler T, Kromer B et al. (2010) Observations and modelling of the global distribution and long-term trend of atmospheric $^{14}CO_2$. Tellus B 62:26–46.

Li M, Hoch G, Körner C (2002) Source/sink removal affects mobile carbohydrates in *Pinus cembra* at the Swiss treeline. Trees 16:331–337.

McCarthy HR, Pataki DE (2010) Drivers of variability in water use of native and non-native urban trees in the greater Los Angeles area. Urban Ecosyst 13:393–414.

McDowell N, Pockman WT, Allen CD et al. (2008) Mechanisms of plant survival and mortality during drought: why do some plants survive while others succumb to drought? New Phytol 178:719–739.

Mooney HA, Hays RI (1973) Carbohydrate storage cycles in two Californian Mediterranean-climate trees. Flora 162:295–304.

Muhr J, Angert A, Negrón-Juárez RI, Muñoz WA, Kraemer G, Chambers JQ, Trumbore SE (2013) Carbon dioxide emitted from live stems of tropical trees is several years old. Tree Physiol 33:743–752.

Pavlik BM, Muick PC, Johnson SG, Popper M (2006) Oaks of California, 6th edn. Evarts J (ed.). Cachuma Press and the California Oak Foundation, 186 pp.

Plavcová L, Jansen S (2015) The role of xylem parenchyma in the storage and utilization of non-structural carbohydrates. In: Hacke UG (ed.), Functional and ecological xylem anatomy. Springer, pp 209–223.

Raessler M (2011) Sample preparation and current applications of liquid chromatography for the determination of non-structural carbohydrates in plants. Trends Analyt Chem 30:1833–1843.

Richardson AD, Carbone MS, Keenan TF, Czimczik CI, Hollinger DY, Murakami P, Schaberg PG, Xu X (2013) Seasonal dynamics and age of stemwood nonstructural carbohydrates in temperate forest trees. New Phytol 197:850–861.

Richardson AD, Carbone MS, Huggett BA, Furze ME, Czimczik CI, Walker JC, Xu X, Schaberg PG, Murakami P (2015) Distribution and mixing of old and new nonstructural carbon in two temperate trees. New Phytol 206:590–597.

Richter A, Wanek W, Werner RA et al. (2009) Preparation of starch and soluble sugars of plant material for the analysis of carbon isotope composition: a comparison of methods. Rapid Commun Mass Spectrom 23:2476–2488.

Rocha AV, Goulden ML, Dunn AL, Wofsy SC (2006) On linking interannual tree ring variability with observations of whole-forest CO_2 flux. Glob Change Biol 12:1378–1389.

Sala A, Woodruff DR, Meinzer FC (2012) Carbon dynamics in trees: feast or famine? Tree Physiol 32:764–775.

Santos G, Ormsby K (2013) Behavioral variability in ABA chemical pretreatment close to the ^{14}C age limit. Radiocarbon 55:534–544.

Schuur EAG, Trumbore SE (2006) Partitioning sources of soil respiration in boreal black spruce forest using radiocarbon. Glob Change Biol 12:165–176.

Sevanto S, McDowell NG, Dickman LT, Pangle R, Pockman WT (2014) How do trees die? A test of the hydraulic failure and carbon starvation hypotheses. Plant Cell Environ 37:153–161.

Sierra C, Müller M, Trumbore SE (2014) Modeling radiocarbon dynamics in soils: SoilR version 1.1. Geosci Model Dev 7:1919–1931.

Snow CH (1903) The principal species of wood: their characteristic properties. John Wiley and Sons, NY.

Soetaert K, Petzoldt T (2010) Inverse modelling, sensitivity and Monte Carlo analysis in R using package FME. J Stat Softw 33:1–28.

Southon J, Santos GM (2007) Life with MC-SNICS. Part II: further ion source development at the Keck carbon cycle AMS facility. Nucl Instrum Methods Phys Res B 259:88–93.

Southon J, Santos G, Druffel-Rodriguez K, Druffel E, Trumbore S, Xu X, Griffin S, Ali S, Mazon M (2004) The Keck Carbon Cycle AMS laboratory, University of California, Irvine: initial operation and a background surprise. Radiocarbon 46:41–49.

Stuiver M, Polach H (1977) Discussion: reporting of radiocarbon data. Radiocarbon 19:355–363.

Tschaplinski TJ, Hanson PJ (2003) Dormant-season nonstructural carbohydrate storage. In: Hanson PJ, Wullschleger SD (eds) North American temperate deciduous forest responses to changing precipitation regimes. Chapter 3 (pp 67–86). Springer, New York, 465 pp.

Vargas R, Trumbore SE, Allen MF (2009) Evidence of old carbon used to grow new fine roots in a tropical forest. New Phytol 182:710–718.

Vieira S, Trumbore S, Camargo PB, Selhorst D, Chambers JQ, Higuchi N, Martinelli LA (2005) Slow growth rates of Amazonian trees: consequences for carbon cycling. Proc Natl Acad Sci USA 102:18502–18507.

Wong BL, Staats LJ, Burfeind AS, Baggett KL, Rye AH (2005) Carbohydrate reserves in *Acer saccharum* trees damaged during the January 1998 ice storm in northern New York. Can J Bot 83:668–677.

Worbes M (2002) One hundred years of tree-ring research in the tropics—a brief history and an outlook to future challenges. Dendrochronologia 20:217–231.

Würth MKR, Peláez-Riedl S, Wright SJ, Körner C (2005) Non-structural carbohydrate pools in a tropical forest. Oecologia 143:11–24.

Xu X, Trumbore SE, Zheng S, Southon JR, McDuffee KE, Luttgen M, Liu JC (2007) Modifying a sealed tube zinc reduction method for preparation of AMS graphite targets: reducing background and attaining high precision. Nucl Instrum Methods Phys Res B 259:320–329.

Xu X, Khosh MS, Druffel-Rodriguez KC, Trumbore SE, Southon JR (2010) Is the consensus value of ANU sucrose (IAEA C-6) too high? Radiocarbon 52:866–874.